Exact NFDM transmission in the presence of fiber-loss

Bajaj, Vinod; Chimmalgi, Shrinivas; Aref, Vahid; Wahls, Sander

DOI
10.1109/JLT.2020.2984041

Publication date
2020

Document Version
Final published version

Published in
Journal of Lightwave Technology

Exact NFDM Transmission in the Presence of Fiber-Loss

Vinod Bajaj, Shrinivas Chimmalgi, Vahid Aref, and Sander Wahls, *Senior Member, IEEE*

***Abstract*—Nonlinear frequency division multiplexing (NFDM) techniques encode information in the so called nonlinear spectrum which is obtained from the nonlinear Fourier transform (NFT) of a signal. NFDM techniques so far have been applied to the nonlinear Schrödinger equation (NLSE) that models signal propagation in a lossless fiber. Conventionally, the true lossy NLSE is approximated by a lossless NLSE using the path-average approach which makes the propagation model suitable for NFDM. The error of the path-average approximation depends strongly on signal power, bandwidth, and the span length. It can degrade the performance of NFDM systems and imposes challenges on designing high data rate NFDM systems. Previously, we proposed the idea of using dispersion decreasing fiber (DDF) for NFDM systems. These DDFs can be modeled by a NLSE with varying-parameters that can be solved with a specialized NFT without approximation errors. We have shown in simulations that complete nonlinearity mitigation can be achieved in lossy fibers by designing an NFDM system with DDF if a properly adapted NFT is used. We reported performance gains by avoiding the aforementioned path-average error in an NFDM system by modulating the discrete part of the nonlinear spectrum. In this article, we extend the proposed idea to the modulation of continuous spectrum. We compare the performance of NFDM systems designed with dispersion decreasing fiber to that of systems designed with a standard fiber with path-average model. Next to the conventional path-average model, we furthermore compare the proposed system with an optimized path-average model in which amplifier locations can be adapted. We quantify the improvement in the performance of NFDM systems that use DDF through numerical simulations.**

***Index Terms*—Fiber-optic communication, nonlinear frequency division multiplexing, nonlinear Fourier transform, dispersion decreasing fiber.**

I. Introduction

THE ability of the nonlinear Fourier transform (NFT) to linearise the lossless nonlinear fiber-optic channel has attracted much research in recent years. An optical pulse propagates through an ideal optical fiber in a complicated manner as dispersive and nonlinear effects act simultaneously on it. This complicated propagation translates into simple rotations in the nonlinear spectrum [1]. As the nonlinear spectrum evolves linearly through nonlinear lossless fiber, the cross-talk among the spectral components is absent. This has led to the emergence of new types of optical fiber transmission technologies where fiber-nonlinearity is no longer seen as an undesired element. Because of the immunity to nonlinear cross-talk and simple equalization, NFT based transmission techniques are seen as interesting approach to mitigate fiber-nonlinearity [2], [3]. The propagation of a pulse in an ideal optical fiber is modeled by the lossless NLSE, which belongs to a certain class of evolution equations, known as integrable evolution equations. The property of integrabilty of the lossless NLSE makes it exactly solvable by NFT [1]. The NFT decomposes a signal into a nonlinear spectrum which consists of two parts: continuous and discrete spectrum. The continuous part consists of continuous spectral functions representing the radiative components of the signal. The discrete part consists of a set of isolated points called eigenvalues and their corresponding spectral values. The discrete part represents the solitonic components of the signal. The absence of interference between these nonlinear spectral components (in an ideal fiber) encourages the idea of encoding information on them and new transmission techniques were proposed known as nonlinear frequency division multiplexing (NFDM) [3]. NFDM systems face several challenges such as complicated noise statistics [4], [5], numerical complexity, and the lack of general efficient optical methods to (de-)multiplex several users in the nonlinear frequency domain [6], [7]. Another, fundamental issue is the loss in optical fibers. The fiber-loss breaks the integrability property of NLSE and hence, the NFT is not exactly applicable. Traditionally in NFDM systems, this challenge is addressed with the path-average model [8], [9], where the lossy propagation of the signal is approximated by lossless propagation in an other fiber (with a path-averaged nonlinear parameter). Many NFDM transmission results have been demonstrated utilizing this model [10]–[14]. An improvement in the accuracy of the path-average model was shown by a shift in the amplifier locations in the link [15], [16]. However, the signal propagation described by the path-average model always deviates from the actual propagation due to the use of approximation. Perfect nonlinearity compensation cannot be achieved even in absence of noise [11]. Further, the approximation errors become stronger when signal power, bandwidth and span length increase [9], [11], [16].

Manuscript received December 6, 2019; revised March 2, 2020 and March 24, 2020; accepted March 24, 2020. Date of publication April 2, 2020; date of current version May 27, 2020. This work was supported in part by the European Union's Horizon 2020 Research and Innovation programme through the FONTE project under Grant 766115, and in part by the European Research Council (ERC) under the European Union's Horizon 2020 Research and Innovation programme under Grant 716669. *(Corresponding author: Vinod Bajaj.)*

Vinod Bajaj, Shrinivas Chimmalgi, and Sander Wahls are with the Delft Center for Systems and Control, Delft University of Technology, 2628 CD Delft, The Netherlands (e-mail: v.bajaj-1@tudelft.nl; s.chimmalgi@tudelft.nl; s.wahls@tudelft.nl).

Vahid Aref is with Nokia Bell-labs, 70435 Stuttgart, Germany (e-mail: vahid.aref@nokia-bell-labs.com).

Color versions of one or more of the figures in this article are available online at http://ieeexplore.ieee.org.

Digital Object Identifier 10.1109/JLT.2020.2984041

In order to avoid the approximation errors associated with the path-average model, we investigated an idea from classical single soliton systems [17]. In these systems dispersion decreasing fiber (DDF) was introduced to prevent soliton broadening in lossy fiber [18]–[22]. These fibers are made such that the balance between the dispersive and nonlinear effects is preserved along the fiber. Furthermore, it has been shown in [23] that a DDF can be approximated efficiently using a fiber with a stepwise dispersion profile. It was found in the study that an n-fold stepwise dispersion profiling provides an equivalent reduction in the errors due to the path-average approximation as an n-fold decrease in the span length. Nevertheless, if a fiber with desired dispersion decreasing profile is designed then its propagation model is exactly integrable and hence can be solved exactly with NFTs [24]. Thus in an NFDM system designed with DDF, the nonlinear and dispersive impairments in the signal introduced during the noiseless propagation can be perfectly mitigated even though there is fiber-loss. An NFDM transmission system designed with DDF requires a suitably adapted NFT. We previously demonstrated such an exact NFDM transmission over DDF using the modulation of the discrete part of the nonlinear spectrum [17].

In this paper, we extend our previous results when the data is modulated on the continuous spectrum. Further, we compliment the previous results of discrete spectrum modulation by comparing the performance of an NFDM system designed using DDF to an NFDM system designed using constant dispersion fiber (CDF), where the parameters of the CDF are chosen in the range of standard non-zero dispersion shifted fiber. We furthermore include the performance of an NFDM system designed using CDF when the location of amplifiers are optimized in the transmission-link. The paper is organized as follows. In Section II, we review the basics of NFDM and the path-average model. In Section III, we discuss the advantages of using DDF in designing NFDM system in the presence of fiber-loss along with the corresponding NFT. Then, in Section IV, we describe the simulation setups and present results for discrete spectrum and continuous spectrum modulation respectively. The paper is concluded in Section V.

II. Basics of NFDM

The propagation of an optical pulse $Q(\ell, t)$ in an ideal lossless single-mode fiber can be modeled by the NLSE [8, Ch. 2.6.2]

$$\frac{\partial Q}{\partial \ell} + i\frac{\beta_2}{2}\frac{\partial^2 Q}{\partial t^2} - i\gamma|Q|^2 Q = 0, \tag{1}$$

where ℓ represents the propagation distance and t is retarded time. The parameters β_2 and γ are the dispersion and nonlinear parameters respectively. Here, we consider the anomalous dispersion case $\beta_2 < 0$. The above equation is integrable and can be solved exactly by NFTs. By a change of variables,

$$u = \frac{Q}{\sqrt{P}}, \quad z = \frac{\ell}{L_D}, \quad \tau = \frac{t}{T_0},$$

where $L_D = \frac{T_o^2}{|\beta_2|}$, $P = \frac{1}{\gamma L_D}$ and T_0 is a free parameter, (1) can be transformed into the normalized form

$$\frac{\partial u}{\partial z} - i\frac{1}{2}\frac{\partial^2 u}{\partial \tau^2} - i|u|^2 u = 0, \quad u = u(z,\tau). \tag{2}$$

The NFT of a vanishing signal $u(z,\tau)$ with respect to (2) is obtained by the solution of the so-called Zakharov-Shabat scattering problem [1]

$$\frac{\partial}{\partial \tau}\begin{pmatrix}\vartheta_1(z,\tau)\\ \vartheta_2(z,\tau)\end{pmatrix} = \begin{pmatrix}-j\lambda & u(z,\tau)\\ -u^*(z,\tau) & j\lambda\end{pmatrix}\begin{pmatrix}\vartheta_1(z,\tau)\\ \vartheta_2(z,\tau)\end{pmatrix} \tag{3}$$

with the boundary condition

$$\begin{pmatrix}\vartheta_1(z,\tau)\\ \vartheta_2(z,\tau)\end{pmatrix} \to \begin{pmatrix}1\\ 0\end{pmatrix}\exp(-j\lambda\tau) \text{ for } \tau \to -\infty. \tag{4}$$

The Jost scattering coefficients are defined as

$$\begin{aligned} a(\lambda, z) &= \lim_{\tau\to+\infty} \vartheta_1(z,\tau)\exp(j\lambda\tau),\\ b(\lambda, z) &= \lim_{\tau\to+\infty} \vartheta_2(z,\tau)\exp(-j\lambda\tau). \end{aligned} \tag{5}$$

The NFT of $u(z,\tau)$, for fixed z, consists of two parts:

1) Continuous Spectrum: For $\lambda \in \mathbb{R}$, now onward denoted by ξ, consisting of spectral functions $\rho_c(\xi) = b(\xi)/a(\xi)$.

2) Discrete Spectrum: For $\lambda \in \mathbb{C}^+$, consisting of eigenvalues λ_j and their corresponding discrete spectral values $\rho_{d,j}$,

$$\left(\lambda_j,\ \rho_{d,j} := b(\lambda_j)/\frac{da}{d\lambda}(\lambda_j)\right),$$

where the eigenvalues are the zeros of $a(\lambda, z)$ with respect to λ in the complex upper half-plane.

The evolution of the signal in the nonlinear Fourier domain with respect to the standard lossless NLSE (2) is given by [1]

$$\begin{aligned} \rho_c(\xi, z) &= \rho_c(\xi, 0)e^{2i\xi^2 z},\\ \rho_{d,j}(\lambda_j, z) &= \rho_{d,j}(\lambda_j, 0)e^{2i\lambda_j^2 z},\\ \lambda_j(z) &= \lambda_j(0). \end{aligned} \tag{6}$$

Eq. (6) implies that the impairments due to the dispersive and nonlinear effects acting simultaneously on a signal can be equalized easily in the nonlinear Fourier domain. Further, the cross-talk due to fiber-propagation is absent among the nonlinear spectral components (6). In NFDM techniques, these spectral components are utilized as data-carriers.

So far, we have considered a lossless fiber but real fibers have non-negligible loss, which can be accounted in (1) by a loss parameter α [8],

$$\frac{\partial Q}{\partial \ell} + i\frac{\beta_2}{2}\frac{\partial^2 Q}{\partial t^2} - i\gamma|Q|^2 Q = -\frac{\alpha}{2}Q. \tag{7}$$

The above equation is not integrable, hence it is not suitable for NFDM. One way to address this issue is by using the path-average model [9]. In the path-average model, the variation in the signal power due to loss is transformed into variations in the nonlinear parameter. Then, by approximating the varying nonlinear parameter with its average value over a span, a lossless fiber model is obtained.

NFDM techniques can be applied to the fiber model obtained using the path-average approach. However, as the model has been derived with an approximation, errors are introduced and complete nonlinearity compensation cannot be achieved even in absence of noise [11]. In the next section, we discuss how by using a suitably designed fiber exact nonlinearity compensation can be achieved even in the presence of loss, assuming that higher order effects in the fiber such as third order dispersion or scattering are negligible.

III. Dispersion Decreasing Fiber and Modified NFT

In order to preserve the integrability property in presence of loss, a fiber can be designed with varying dispersion and/or nonlinear parameter profile [18]. As these two parameters are linked with the effective core radius of fiber, a fiber with a desired profile can be manufactured practically by tapering the optical fiber during the draw process [8, Ch. 9.3.1], [20], [21]. In this paper, we assume a simplified approximate relation between the effective core radius r (in μm) and the dispersion parameter β_2 that was given in [18],[1]

$$r(\beta_2) = (-\beta_2/\kappa + 20)/8, \tag{8}$$

where $\kappa = \lambda_0^2/2\pi c \times 10^{-6}$ and λ_0 and c are the wavelength and speed of light in free space respectively. The nonlinear parameter depends on the effective core radius as follows [8 Ch. 2.6.2][1]

$$\gamma = 2n_2/(\lambda_0 r^2), \tag{9}$$

where n_2 is the nonlinear-index coefficient. Hence, by controlling the radius r, a fiber with variable dispersion parameter $\beta_2(\ell) = \beta_2(0)D(\ell)$ and a variable nonlinear parameter $\gamma(\ell) = \gamma(0)R(\ell)$ can be designed. The propagation of an optical pulse $Q(\ell, t)$ in such a fiber is then given by [24]

$$\frac{\partial Q}{\partial \ell} + i\frac{\beta_2(0)D(\ell)}{2}\frac{\partial^2 Q}{\partial t^2} - i\gamma(0)R(\ell)|Q|^2 Q = -\frac{\alpha}{2}Q. \tag{10}$$

The above equation can be transformed as before, but with $L_D = \frac{T_0^2}{|\beta_2(0)|}$ and $P = \frac{1}{\gamma(0)L_D}$, into the normalized form

$$\frac{\partial q}{\partial z} - i\frac{D(z)}{2}\frac{\partial^2 q}{\partial \tau^2} - iR(z)|q|^2 q = -\frac{\alpha L_D}{2}q. \tag{11}$$

It was shown in [24] that the above equation can be solved exactly via NFT if

$$\alpha L_D = -\frac{R(z)D'(z) - R'(z)D(z)}{R(z)D(z)}, \tag{12}$$

where the prime denotes differentiation.

The NFT of $q(z,\tau)$ with respect to (11) is now defined as the conventional NFT of the signal $u(z,\tau) = \sqrt{\frac{R(z)}{D(z)}}q(z,\tau)$. The reader is referred to Appendix A for a detailed description. The evolution of the signal in the nonlinear Fourier domain with respect to (11) is given by

$$\begin{aligned}\rho_c(\xi, z) &= \rho_c(\xi, 0)e^{2i\xi^2 \int_0^z D(\zeta)d\zeta},\\ \rho_{d,j}(\lambda_j, z) &= \rho_{d,j}(\lambda_j, 0)e^{2i\lambda_j^2 \int_0^z D(\zeta)d\zeta},\\ \lambda_j(z) &= \lambda_j(0).\end{aligned} \tag{13}$$

The above relation enables us to recover the signal impaired simultaneously with loss, dispersion and nonlinearity. In order to satisfy (12), the required dispersion profile has to satisfy

$$\frac{\beta_2(\ell)}{\gamma(\ell)} = ae^{-\alpha\ell}, \tag{14}$$

where $a = \frac{\beta_2(0)}{\gamma(0)}$. By combining (8), (9) and (14), we arrive at[1]

$$8r^3(\ell)\kappa - 20\kappa r^2(\ell) + \frac{2an_2}{\lambda_0}e^{-\alpha\ell} = 0. \tag{15}$$

If equation (15) is written as

$$c_3\, r^3 + c_2\, r^2 + c_1\, r + c_0 = 0. \tag{16}$$

Then for our case ($\kappa > 0$ and $a < 0$), the coefficients are real and $c_3 = 8\kappa > 0$, $c_2 = -20\kappa < 0$, $c_1 = 0$, $c_0 = 2an_2/\lambda_0 < 0$ and discriminant $\Delta = 18c_3c_2c_1c_0 - 4c_2^3c_0 + c_2^2c_1^2 - 4c_3c_1^3 - 27c_3^2c_0^2 < 0$. Thus, the equation will always have one real root and two complex conjugate roots [25]. The real root is positive and corresponds to the radius that satisfies equation (15). The real-valued solution at different ℓ provides us the distance dependent effective core radius. Once the radius $r(\ell)$ is known we can find $\beta_2(\ell)$ and $\gamma(\ell)$ from (8) and (9) respectively.

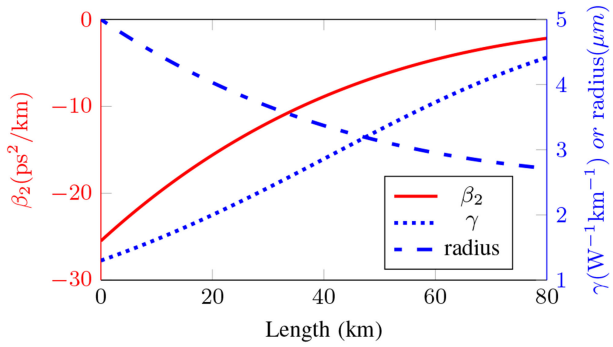

Fig. 1. DDF parameters for a single span as used in the simulations.

We chose realistic values of fiber parameters and controlled the effective core radius to achieve the desired profile for fiber-loss of 0.2 dB/km as shown in Fig. 1. The value for the nonlinear-index coefficient n_2 and λ_0 was taken as $2.52 \times 10^{-20}\ \mathrm{m}^2/\mathrm{W}$ and 1.55 μm respectively. The dispersion parameter β_2 is varied from $-25\ \mathrm{ps}^2/\mathrm{km}$ to $-2.17\ \mathrm{ps}^2/\mathrm{km}$, while the nonlinear parameter is varied from 1.3 $\mathrm{W}^{-1}\mathrm{km}^{-1}$ to 4.4 $\mathrm{W}^{-1}\mathrm{km}^{-1}$. Here, the effective core radius of fiber is decreased slowly over 80 km length so that the radiation losses are expected to be negligible [26]. Third order dispersion was not implemented since realistic values around $\beta_3 = 0.05\ \mathrm{ps}^3/\mathrm{km}$ are expected to be insignificant in our case due to the high average dispersion parameter and nanosecond pulse durations [26].

[1]Equation (15) above differs slightly from the results reported in [17] because there were typos in the equations (2), (3) and (8) of [17].

TABLE I
FIBER PARAMETERS USED IN SIMULATIONS

Fiber type	CDF	DDF
α (dB/km)	0.2	0.2
β_2 (ps^2/km)	-6.75	-25 to -2.17
γ (1/W/km)	1.3	1.3 to 4.4

It must be noted that the integrability of the channel is still preserved in a link designed using DDF where each span consists of DDF followed by an noiseless amplifier with its gain equal to span-loss. In such a link, at an amplifier not only the gain is added, but also the fiber parameters (β_2, γ) change as a new span starts. In the normalized domain, these two effects cancel each other and the integrability of the channel is preserved.

IV. SIMULATION SETUP AND RESULTS

In this section, we numerically compare the performance of NFDM systems in DDF to that in CDF. The parameters of the DDF are shown in Fig. 1 as described earlier. Due to the different fiber characteristics, it is not obvious how fair the two setups can be compared. The parameters of the CDF were chosen in such a way that both systems have the same power, bandwidth and time duration at the transmitter,[2]. This requires that the time-scale parameter T_0 and power-scale parameter P, which scales the normalized signal before transmission should be the same for both systems. The obtained CDF parameters are summarized in Table I and are very close to realistic parameters of standard non-zero dispersion shifted fibers. It is worth mentioning that for the DDF case, the normalization length L_D is smaller and the overall dispersion and nonlinearity is higher.The simulations were carried out with the open-source software environment NFDMlab [27], which uses FNFT [28], a software library to compute NFTs and INFTs. We compare the performance between the NFDM systems designed with the two fibers, CDF and DDF. First we evaluate the NFDM systems using discrete spectrum modulation and later using continuous spectrum modulation.

1) NFDM With Discrete Spectrum Modulation: We considered the multi-soliton transceiver presented in [12], in which the spectral values $\rho_{d,j}$ of seven eigenvalues λ_j were modulated independently with QPSK. The system parameter were kept the same as presented in [12] unless otherwise stated.

The simulation setup is shown in Fig. 2. At the transmitter, randomly generated QPSK symbols were modulated on the discrete spectral values of the corresponding seven eigenvalues given in [12] and shown in Fig. 3. Then the time-domain multi-soliton pulse was obtained with the inverse NFT (INFT) operation. The duration of the normalized multi-soliton pulse was set to 18π in order to avoid truncation effects and pulse-overlap during propagation. The normalized multi-soliton pulse is then scaled using the fiber parameters and time-scale parameter T_0. T_0 controls the duration of de-normalized pulse and hence the transmit power. A train of 1023 pulses was transmitted through the link

[2]It may be interesting to see a comparison of these systems designed in other possible ways. In our prior work[17] a different comparison was carried out.

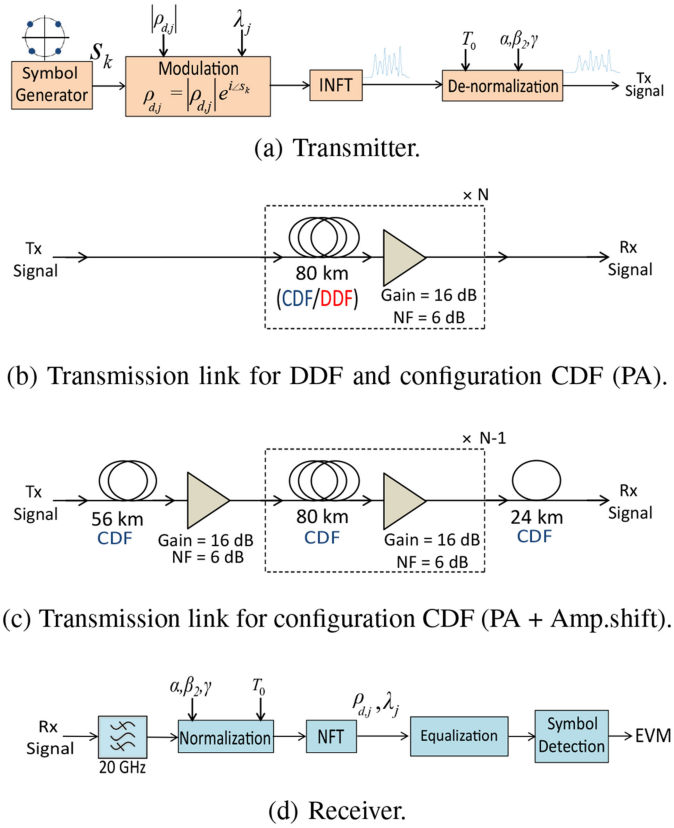

Fig. 2. Simulation setup of NFDM system with discrete spectrum modulation.

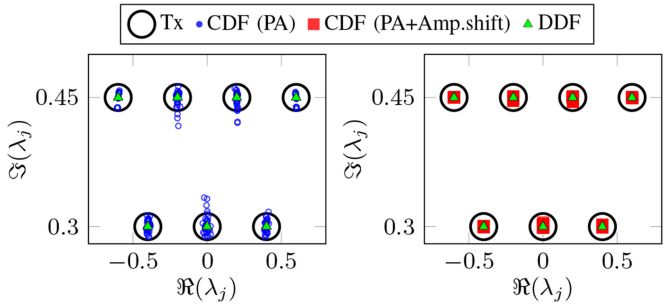

Fig. 3. Transmitted and received eigenvalues for 8×80 km noiseless transmission at 2.82 dBm transmit power (left) and 4.7 dBm transmit power (right).

for each evaluation. For the case of NFDM system designed using CDF, we considered two types of link configurations. Fig. 2(b) shows the transmission link for the first configuration (referred as CDF–PA). In this transmission link, each span in the link consists of 80 km fiber followed by an Erbium-doped fiber amplifier (EDFA) to compensate the span-loss of 16 dB. The same link configuration was used for the NFDM system designed with DDF. The second configuration of link, shown in Fig. 2(c), is same as the first one except for the first and the last spans which have different lengths (referred as CDF–PA+Amp-shift). The lengths of the first and the last span were optimized according to the analysis in [16]. It was shown in [16] that the approximation error of path-average model is minimized at those optimal lengths. The transmit power in the second configuration refers to the power at the amplifier outputs. The noise figure of

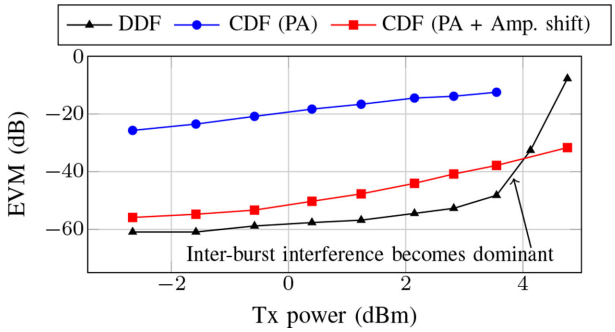

Fig. 4. Discrete spectrum modulation: EVM over transmit power for 16×80 km noiseless transmission.

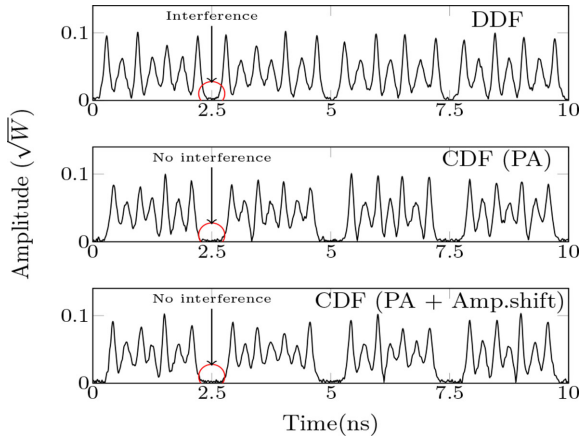

Fig. 5. Signal after 16×80 km transmission over different link-configurations (at transmit power of 2.8 dBm). The pulses spread more for the case of DDF, resulting into interference among them.

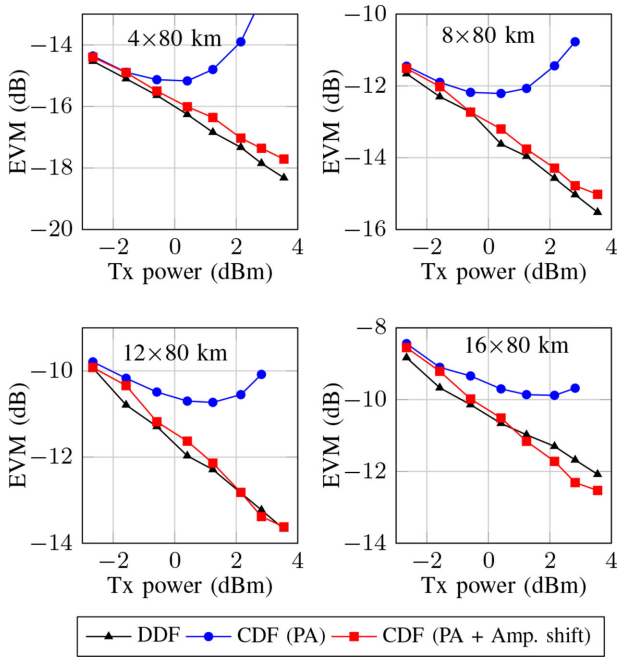

Fig. 6. Discrete spectrum modulation : EVM over transmit power for different transmission distances.

the EDFAs was set to 6 dB in both link configurations. The fiber propagation was simulated using a split-step Fourier method. At the receiver (shown in Fig. 2(d)), the signal was filtered to remove out of band noise. After normalization, the signal was then equalized in the nonlinear Fourier domain using (6) for CDF and (13) for DDF. The QPSK symbols were demodulated from the spectral values of the eigenvalues. Finally, performance is measured in terms of the error vector magnitudes (EVMs) of received symbols.

Fig. 3 shows the 7-eigenvalues transmitted over noiseless 640 km link and the corresponding received eigenvalues for the case of NFDM systems designed using DDF and CDF. We can see that in the absence of noise the NFDM system designed using DDF is exact and preserves the eigenvalues while there is fluctuation in the received eigenvalues of the NFDM system designed using CDF due to the involved path-average approximation. Fig. 4 shows EVM over transmit power for 16×80 km noiseless transmission. In the low transmit power region, the performance of the NFDM system designed using DDF is limited only by the accuracy of the numerical approximations. The performance of the NFDM systems designed using CDF (the other two cases) is mainly limited by errors due to the path-average approximation. We also observe that the NFDM system with CDF (PA + Amp. shift) configuration performs very close to the performance of the NFDM system designed using DDF. However, EVM for NFDM system with CDF (PA + Amp. shift) configuration is rising with increase in power. The EVM for the NFDM system designed using DDF is rising very slowly and then there is a sudden steep rise. This steep rise happens at higher powers (shorter pulse durations) where pulses start to overlap for DDF case due to the following reason.

Remark: The magnitude of the dispersion parameter of the DDF ($|\beta_2(0)|$) at the beginning of the span is larger than the corresponding value of the CDF. Thus, the normalization length ($L_D = T_0^2/|\beta_2(0)|$) of the NFDM system designed using DDF is smaller compared to the other two NFDM systems for a given transmit power. This means that the multi-soliton pulses transmitted over DDF evolves over a longer normalized distance (link length$/L_D$). This results into the spreading of the individual pulses beyond its allocated duration at 16×80 km as shown in Fig. 5, causing interference with neighbouring pulses. This interference is the reason for the degraded performance in the NFDM system designed using DDF at higher power (smaller pulse-duration). However, the other two NFDM systems will also face the inter-pulse interference at longer transmission distances or higher power.

In order to visualize the error due to the path-average approximation in presence of noise, the EVM is plotted in terms of the transmit power for different transmission distances in Fig. 6. For the NFDM system designed using CDF that uses the configuration CDF–PA, the EVM initially decreases with transmit power due to increase in effective signal to noise power ratio (SNR). But after a threshold transmit power, the approximation error due to the path-average model dominates and hence, the EVM starts rising with transmit power. For the NFDM system with CDF–PA+Amp-shift configuration, we did not observe any rise in the EVM in the simulated power range. The NFDM

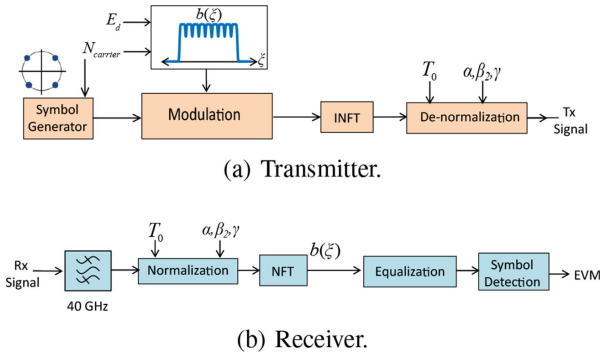

Fig. 7. Simulation setup of NFDM system with continuous spectrum modulation. The transmission link is the same as described before in Fig. 2(b), (c).

scheme that uses DDF performs slightly better than the NFDM scheme that uses CDF–PA+Amp-shift configuration except for the 16×80 km transmission. For 16×80 km transmission in DDF case, the pulses start overlapping at higher powers due to the reason explained earlier. We observe a large gain of up to ≈3 dB in the EVM for 640 km transmission over DDF in comparison to the NFDM system designed with CDF–PA configuration. We also observe that the NFDM system designed with CDF–PA+Amp-shift configuration performs as good as the system designed with DDF in this example, which however has been designed to keep the path-average approximation error small. In the next example we observe much higher gains in the NFDM system designed with DDF.

2) NFDM With Continuous Spectrum Modulation: We considered the NFDM system with b-modulation presented in [29] to modulate continuous spectrum. In b-modulation, the information is modulated on the b-coefficient (5) instead of spectral function $\rho_c(\xi)$. One advantage of b-modulation is that it is easier to control the signal duration using b-modulation in comparison to spectral function $\rho_c(\xi)$ modulation [29], [30]. Another advantage is that the noise impact on the b-coefficient is less severe than the reflection coefficient [31]. The simulation setup of NFDM system is shown in Fig. 7. The nonlinear spectrum consists of nine flat-top shaped $b(\xi)$ carriers with carrier spacing of 15 (in the normalized NFT domain). The average energy of each carrier is controlled by an energy per carrier parameter E_d, which in turn controls the transmit power. Each carrier is modulated with randomly generated QPSK symbols. Then, the INFT operation is performed to obtain time-domain signal with a normalized duration of 4.5. The time-domain pulse is then de-normalized using the fiber parameters and a time scale parameter T_0 of 1.25 ns. A train of 127 pulses is then transmitted through the link. The net data rate and signal bandwidth were 3.2 Gb/s and approximately 40 GHz respectively. The transmission link configurations are the same as described earlier in the case of discrete spectrum modulation and are shown in Fig. 2(b), (c). At the receiver, the signal is filtered and normalized. After the NFT operation the b-coefficients are obtained, which are then equalized using (6) for CDF and (13) for DDF. Finally, the symbols are detected from the $b(\xi)$ carriers and EVMs were computed for different transmission lengths and transmit powers controlled by E_d.

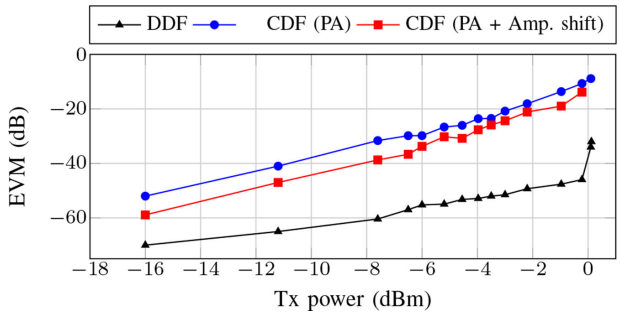

Fig. 8. Continuous spectrum modulation: EVM over transmit power for 16×80 km noiseless transmission.

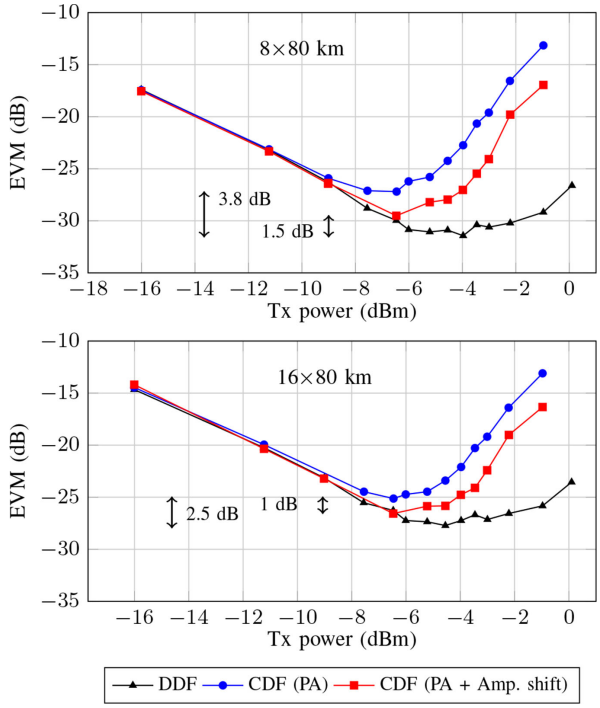

Fig. 9. Continuous spectrum modulation : EVM over transmit power for different transmission distances.

It must be noted that as the magnitude of b-coefficient cannot be greater than one, we have an upper limit on the carrier energy E_d [29], and thus on the transmit power [32]. It was shown theoretically in [32] that the system in [29] cannot exceed a finite power limit. Fig. 8 shows EVM over transmit power for 16×80 km noiseless transmission. We see that EVM for the NFDM system that uses DDF is significantly lower than the other two NFDM systems. In all three NFDM systems, the EVM increases with increase in transmit power. However, the rise in the EVMs for the NFDM systems that use CDF is steeper, which is mainly due to the errors from the path-average approximation. The rise in EVMs for the NFDM system designed using DDF is purely from the accuracy of numerical approximations. At higher power, we get closer to the aforementioned finite power limit and numerical errors occur which is visible for the case of DDF. The b-modulator is prone to breakdown in this region. Fig. 9 shows EVM over transmit power for the case of transmission in the presence of noise. The additive noise increases

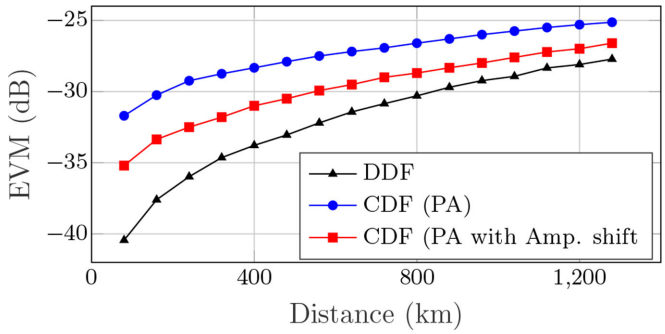

Fig. 10. EVMs over transmission reach at optimal transmit powers.

signal power slightly during transmission. Close to the power bound, this increase in signal power due to the noise is enough to push the received signal outside the range of the b-modulator (in this case the energy gets transferred into discrete spectrum that are not accounted for in the receiver). Thus, the impact of noise becomes severe in the higher power region when the signal approaches the aforementioned finite power limit. This results in the rise in the EVMs of all the considered NFDM systems in the high power region. In Fig. 9, the errors due to the path-average approximation are clearly visible. We can see that for 8×80 km transmission, EVM improves with increasing transmit power but after a threshold the EVM for CDF starts degrading, as the path-average error increased at higher power. Further, we see that approximation error in the path-average model is reduced by the amplifier-shift, hence the NFDM system that uses CDF–PA+Amp-shift configuration has better performance than CDF–PA. The performance of DDF improves with transmit power till -5 dBm, thereafter EVM degrades which is a result of the b-saturation effect. A similar trend is observed for the case of 16×80 km transmission. Fig. 10 shows the minimum EVMs obtained at the corresponding distances for all of the three NFDM systems. We obtained EVM gains of approx. 3.8 dB and 1.5 dB at 640 km with respect to path-average without amplifier-shift and path-average with amplifier-shift respectively. At 1280 km, these gains reduce to 2.5 dB and 1 dB respectively.

In this section, we compared NFDM systems in order to highlight potential advantages of using DDF in NFDM systems. The systems were designed to ensure the system parameters such that the transmitter requirements (bandwidth, power and burst duration) are identical for all three systems. Our comparisons thus isolate and highlight the differences arising solely from choosing DDF instead of CDF. For the chosen system parameters, we also observe that time-spreading of bursts is smaller for the NFDM systems designed using CDF in comparison to the NFDM systems designed using DDF. This difference in time-spreading comes from the fact that the dispersion and nonlinear parameters of CDF and DDF are different. Thus, a smaller guard time interval could be allocated for the NFDM systems designed using CDF, resulting in higher spectral efficiency. A comparison between NFDM systems designed using DDF and CDF independently optimized to maximize performance (bit rate/spectral efficiency) would be an interesting next step.

V. Conclusion

We have presented numerical results for exact NFDM transmission by discrete and continuous spectrum modulation over lossy fiber. We have shown that by using a suitably designed fiber together with an adapted NFT, the approximation error from the path-average model can be avoided. We applied this approach for the case of fiber-links with EDFA based amplification. For discrete spectrum modulation, the NFDM system designed with DDF has EVM gains of up to 3 dB and 2 dB at 640 km and 1280 km respectively in comparison to the NFDM system with path-average model. The EVM performance of the NFDM system with path-average model and amplifier shifts was close to performance of NFDM system with DDF. For the continuous spectrum modulation case, by using DDF, we obtained EVM improvements of approximately 3.8 dB and 2.5 dB for 640 km and 1280 km transmission respectively in comparison to CDF with path-average model. By shifting the amplifiers to optimum locations for the path-average approximation, the gain obtained is approximately 1.5 dB and 1 dB respectively. We observed through simulations that in the presence of fiber-loss, the NFDM systems designed using DDF have clear performance advantage over the NFDM systems designed using CDF for the case of discrete as well as continuous spectrum modulation. It must be noted that the performance-gain obtained in an NFDM system designed with DDF depends on system design parameters. An NFDM system which uses a path-average model will have degraded performance at higher transmit power, bandwidth and longer span, and hence, the gains of employing DDF increase further.

Appendix A
Nonlinear Fourier Transform for DDF

It was shown in [24, Section 3] that if (12) is satisfied, the propagation model given by (11) can be solved with suitable NFTs. In order to compute and evolve the NFT with respect to (11), the following set of linear equations have to be solved [24]

$$\vartheta_\tau = \begin{pmatrix} -j\lambda & \sqrt{\frac{R(z)}{D(z)}}q \\ -\sqrt{\frac{R(z)}{D(z)}}q^* & j\lambda \end{pmatrix}\vartheta, \tag{17}$$

$$\vartheta_z = \begin{pmatrix} -jD(z)\lambda^2 + j\frac{R(z)}{2}|q|^2 & \sqrt{R(z)D(z)}(\lambda q + \frac{j}{2}q_\tau) \\ \sqrt{R(z)D(z)}(\lambda q^* + \frac{j}{2}q_\tau^*) & jD(z)\lambda^2 - jR(z)|q|^2 \end{pmatrix}\vartheta. \tag{18}$$

where $q = q(z,\tau)$, λ is an eigenvalue and ϑ is an eigenvector of the eigenvalue problem (17). Here, the subscript denotes differentiation with the corresponding variable.

From (3), (17) and [2, equation (16)], it is clear that computing the NFT with respect to (11) is same as computing the conventional NFT (with respect to (2)) with the potential $q(z,\tau)$ scaled by a factor of $\sqrt{\frac{R(z)}{D(z)}}$. The evolution of the nonlinear spectrum is described with respect to (18). Following [2, equation (24)], one finds that the evolution of nonlinear spectrum is given by the rotation described in (13).

REFERENCES

[1] V. E. Zakharov and A. B. Shabat, "Exact theory of two-dimensional self- focusing and one-dimensional self-modulation of waves in nonlinear media," *Sov. Phys. JETP*, vol. 34, pp. 62–69, 1972.

[2] M. I. Yousefi and F. R. Kschischang, "Information transmission using the nonlinear Fourier transform, part I: Mathematical tools," *IEEE Trans. Int. Theory*, 60, no. 7, pp. 4312–4328, Jul. 2014.

[3] M. I. Yousefi and F. R. Kschischang, "Information transmission using the nonlinear fourier transform, part III: Spectrum modulation," *IEEE Trans. Int. Theory*, vol. 60, no. 7, pp. 4346–4369, Jul. 2014.

[4] S. Civelli, E. Forestieri, and M. Secondini, "Why noise and dispersion may seriously hamper nonlinear frequency-division multiplexing," *IEEE Photon. Technol. Lett.*, vol. 29, no. 16, pp. 1332–1335, Aug. 2017.

[5] H. Bülow, V. Aref, and L. Schmalen, "Modulation on discrete nonlinear spectrum: Perturbation sensitivity and achievable rates," *IEEE Photon. Technol. Lett.*, vol. 30, no. 5, pp. 423–426, Mar. 2018.

[6] J. Koch, S. Li, and S. Pachnicke, "Transmission of higher order solitons created by optical multiplexing," *J. Lightw. Technol.*, vol. 37, no. 3, pp. 933–941, Feb. 2019.

[7] E. Bidaki and S. Kumar, "Nonlinear Fourier transform using multistage perturbation technique for fiber-optic systems," *J. Opt. Soc. America B*, vol. 35, pp. 2286–2293, 2018.

[8] G. P. Agrawal, *Fiber-Optic Commun. Systems*, 4th ed. New York, NJ, USA: Wiley, 2010.

[9] A. Hasegawa and Y. Kodama, "Guiding-center soliton in optical fibers," *Opt. Lett.*, vol. 15, pp. 1443–1445, 1990.

[10] J. E. Prilepsky, S. A. Derevyanko, K. J. Blow, I. Gabitov, and S. K. Turitsyn, "Nonlinear inverse synthesis and eigenvalue division multiplexing in optical fiber channels," *Phys. Rev. Lett*, vol. 113, 2014, Art. no. 013901.

[11] S. T. Le, J. E. Prilepsky, and S. K. Turitsyn, "Nonlinear inverse synthesis technique for optical links with lumped amplification," *Opt. Express*, vol. 23, pp. 8317–8328, 2015.

[12] H. Bülow, V. Aref, and W. Idler, "Transmission of waveforms determined by 7 eigenvalues with PSK-modulated spectral amplitudes," in *Proc. Eur. Conf. Optical Commun.*, Duesseldorf, Germany, 2016, pp. 1–3.

[13] S. K. Turitsyn *et al.*, "Nonlinear Fourier transform for optical data processing and transmission: Advances and perspectives," *Optica*, vol. 4, no. 3, pp. 307–322, 2017.

[14] V. Aref and H. Buelow, "Design of 2-soliton spectral phase modulated pulses over lumped amplified link," in *Proc. Eur. Conf. Opt. Commun.*, Dusseldorf, Germany, 2016, pp. 1–3.

[15] W. Forysiak, N. J. Doran, F. M. Knox, and K. J. Blow, "Average soliton dynamics in strongly perturbed systems," *Opt. Commun.*, vol. 117, no. 1–2, pp. 65–70, 1995.

[16] M. Kamalian, J. E. Prilepsky, S. T. Le, and S. K. Turitsyn, "On the design of NFT-based communication systems with lumped amplification," *J. Lightw. Technol.*, vol. 35, pp. 5464–5472, Dec. 2017.

[17] V. Bajaj, S. Chimmalgi, V. Aref, and S. Wahls, "Exact nonlinear frequency division multiplexing in lossy fibers," in *Proc. Eur. Conf. Opt. Commun.*, Dublin, Ireland, 2019, pp. 1–3.

[18] K. Tajima, "Compensation of soliton broadening in nonlinear optical fibers with loss," *Opt. Lett.*, vol. 12, no. 1, pp. 54–56, 1987.

[19] H. H. Kuehl, "Solitons on an axially nonuniform optical fiber," *J. Opt. Soc. America B*, vol. 5, no. 3, pp. 709–713, 1988.

[20] S. V. Chernikov and P. V. Mamyshev, "Femtosecond soliton propagation in fibers with slowly decreasing dispersion," *J. Opt. Soc. America B*, vol. 8, no. 8, pp. 1633–1641, 1991.

[21] V. A. Bogatyrev *et al.*, "A single-mode fiber with chromatic dispersion varying along the length," *J. Lightw. Technol.*, vol. 9, no. 5, pp. 561–566, May 1991.

[22] E. M. Dianov, P. V. Mamyshev, A. M. Prokhorov, and S. V. Chernikov, "Generation of a train of fundamental solitons at a high repetition rate in optical fibers," *Opt. Lett.*, vol. 14, no. 18, pp. 1008–1010, 1989.

[23] W. Forysiak, F. M. Knox, and N. J. Doran, "Average soliton propagation in periodically amplified systems with stepwise dispersion-profiled fiber," *Opt. Lett.*, vol. 19, no. 3, pp. 174–176, 1994.

[24] V. N. Serkin and T. L. Belyaeva, "Optimal control of optical soliton parameters: Part 1. The Lax representation in the problem of soliton management," *Quantum Electron.*, vol. 31, no. 11, pp. 1007–1015, 2001.

[25] R. S. Burington, *Handbook of Mathematical Tables and Formulas*, 5th ed. New York, NY, USA: McGraw-Hill, pp. 6–9, 1973.

[26] G. H. M. van Tartwijk, R. J. Essiambre, and G. P. Agrawal, "Dispersion-tailored active-fiber solitons," *Opt. Lett.*, vol. 21, no. 24, pp. 1978–1980, 1996.

[27] M. Brehler, C. Mahnke, S. Chimmalgi, and S. Wahls, "NFDM-Lab: Simulating nonlinear frequency division multiplexing in python," *Proc. Opt. Fiber Commun. Conf. Exhib.*, San Diego, CA, USA, 2019, pp. 1–3.

[28] S. Wahls and S. Chimmalgi and P. J. Prins, "FNFT: A software library for computing nonlinear fourier transforms," *J. Open Source Softw.*, vol. 3, no. 23, pp. 597.1–597.2, 2018.

[29] T. Gui, G. Zhou, C. Lu, A. P. T. Lau, and S. Wahls, "Nonlinear frequency division multiplexing with *b*-modulation: Shifting the energy barrier," *Opt. Express*, vol. 26, pp. 27978–27990, 2018.

[30] S. Wahls, "Generation of time-limited signals in the nonlinear fourier domain via *b*-modulation," in *Proc. Eur. Conf. Opt. Commun.*, 2017, pp. 1–3.

[31] X. Yangzhang, V. Aref, S. T. Le, H. Buelow, D. Lavery, and P. Bayvel, "Dual-polarization non-linear frequency-division multiplexed transmission with *b*-modulation," *J. Lightw. Technol.*, vol. 37, no. 6, pp. 1570–1578, Mar. 2019.

[32] S. Chimmalgi and S. Wahls, "Theoretical analysis of maximum transmit power in a *b*-modulator," in *Proc. Eur. Conf. Opt. Commun.*, Dublin, Ireland, 2019, pp. 1–3.